SIM&TEC

Simulación y Tecnología

Simulation and Technology

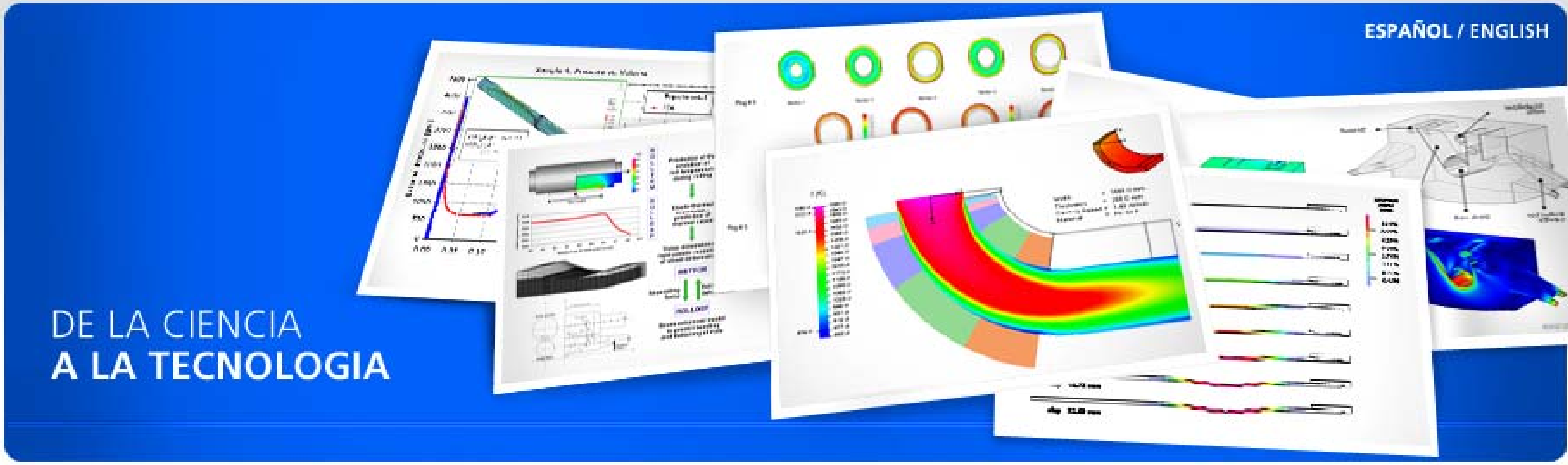

Advanced Topics in Computational Solid Mechanics. Industrial Applications

Section 7: Modeling of Bulk Metal Forming Processes: The Flow Formulation Industrial Applications

Eduardo N. Dvorkin

Stanford University
Mechanical Engineering
Winter Quarter 2010

Steel Pipes Manufacturing Process (1)

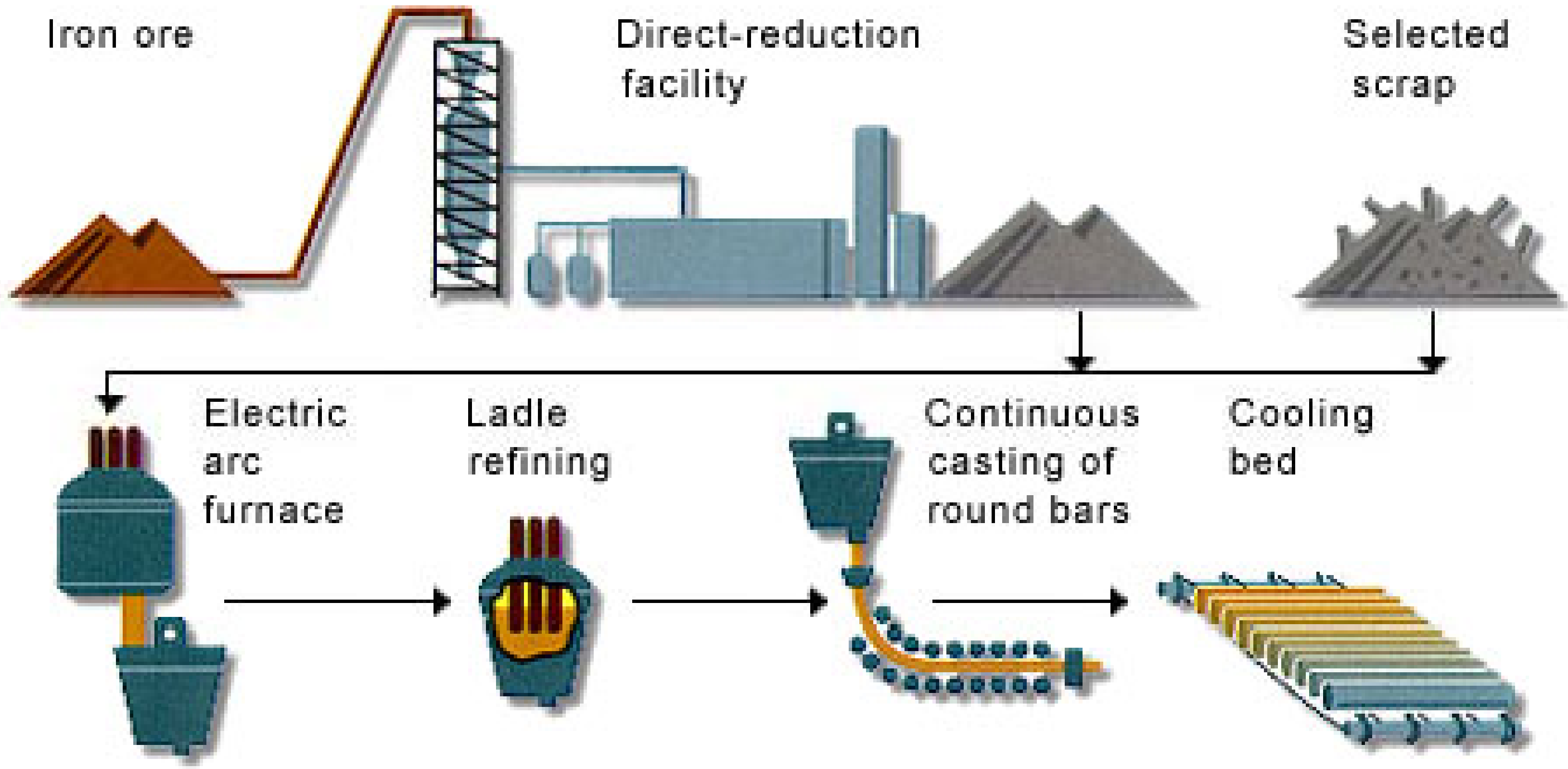

Steel Pipes Manufacturing Process (2)

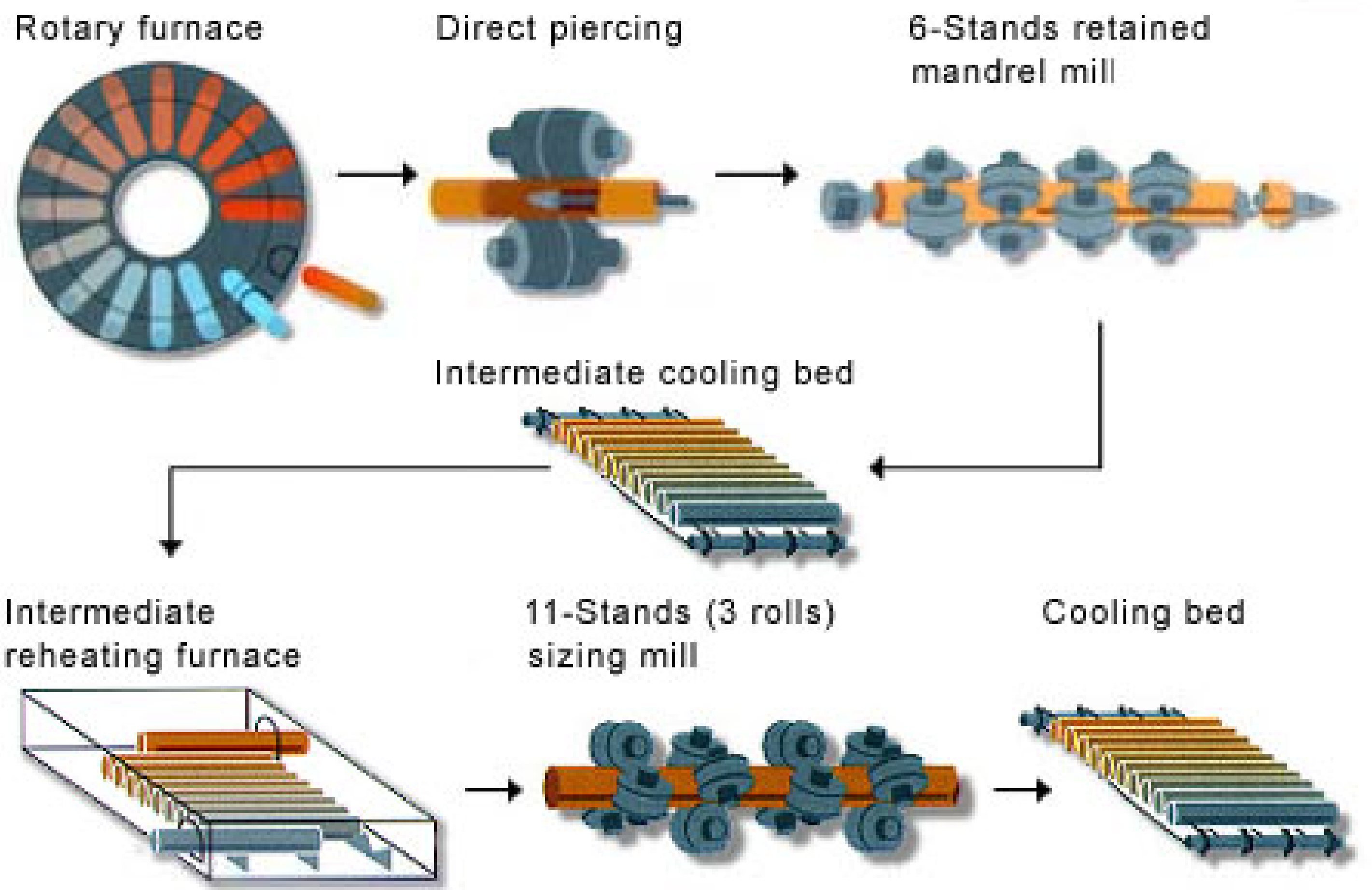

Steel Pipes Manufacturing Process (3)

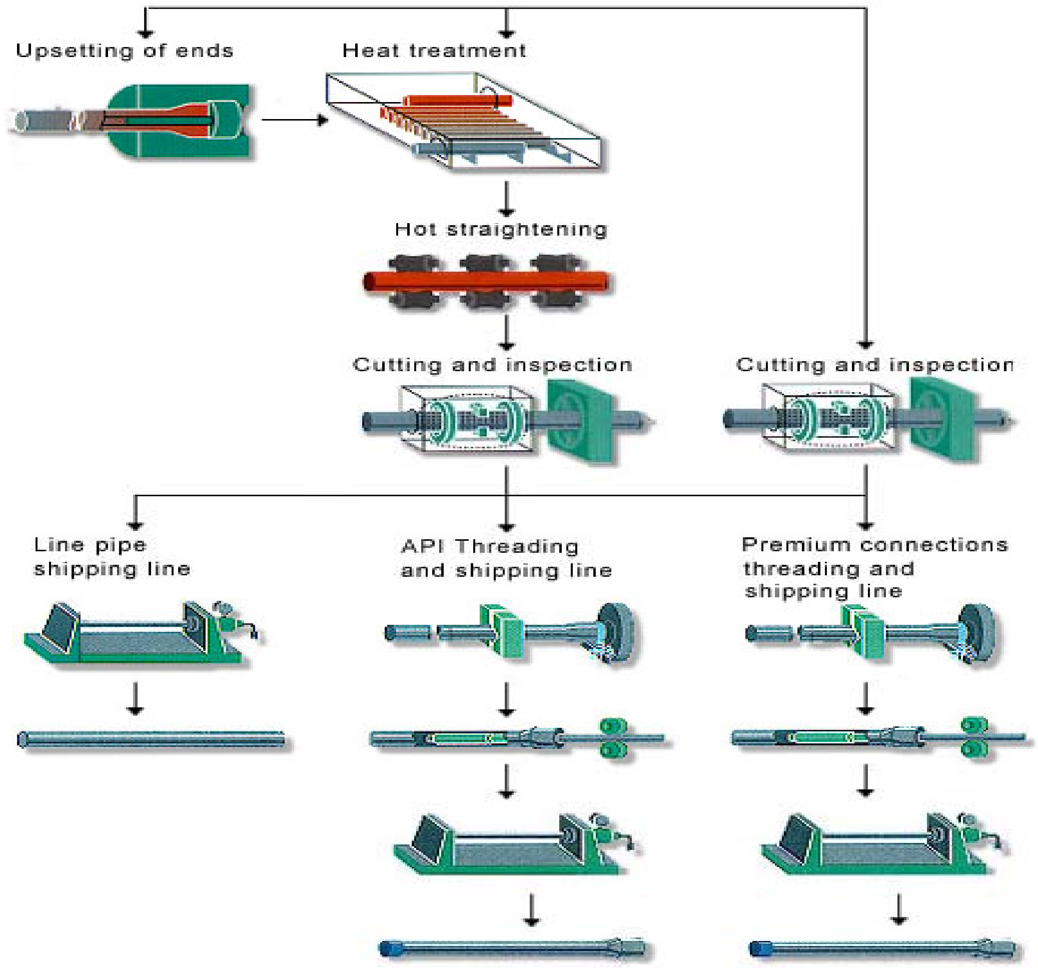

Steel Coils Manufacturing Process (1)

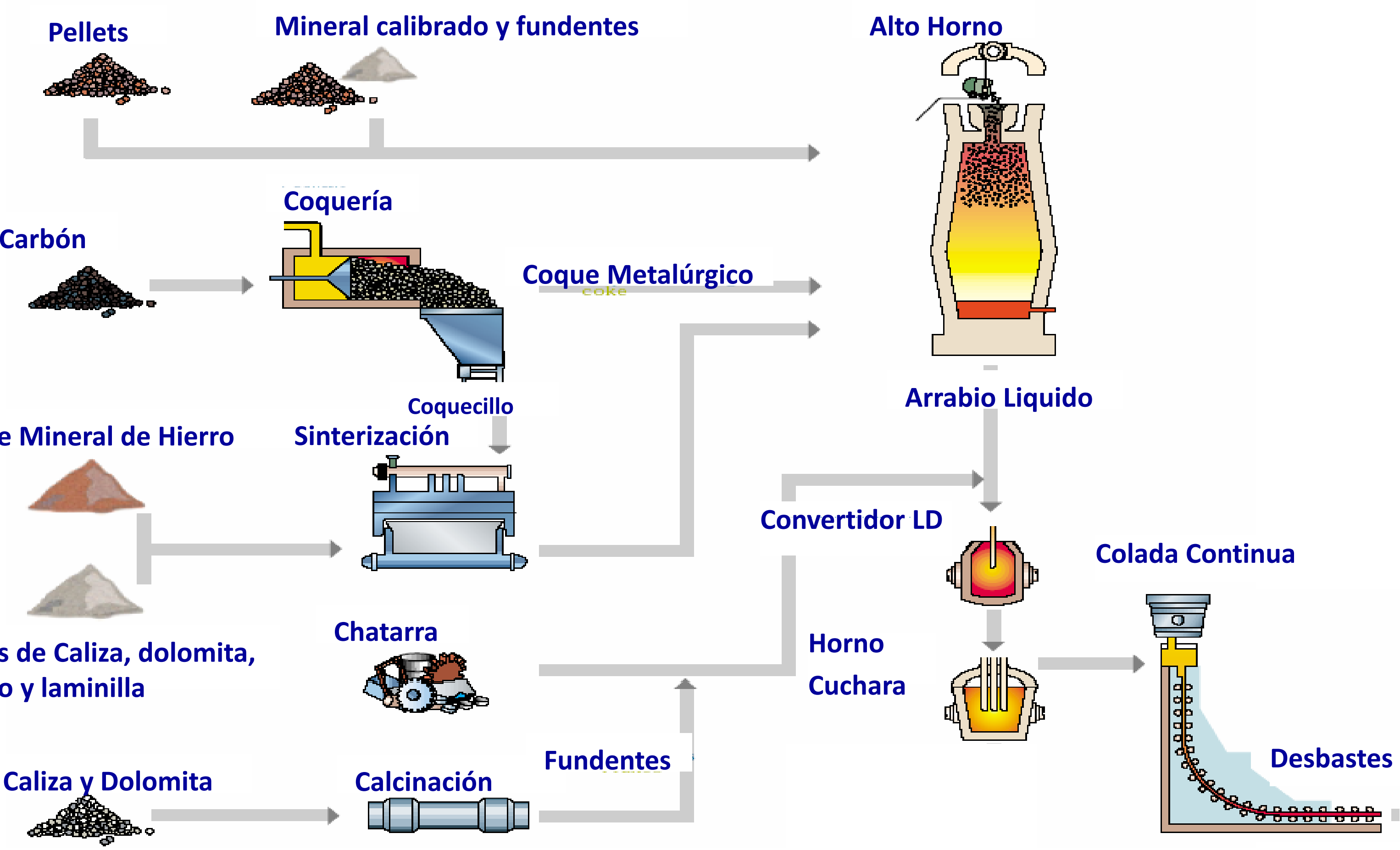

Steel Coils Manufacturing Process (2)

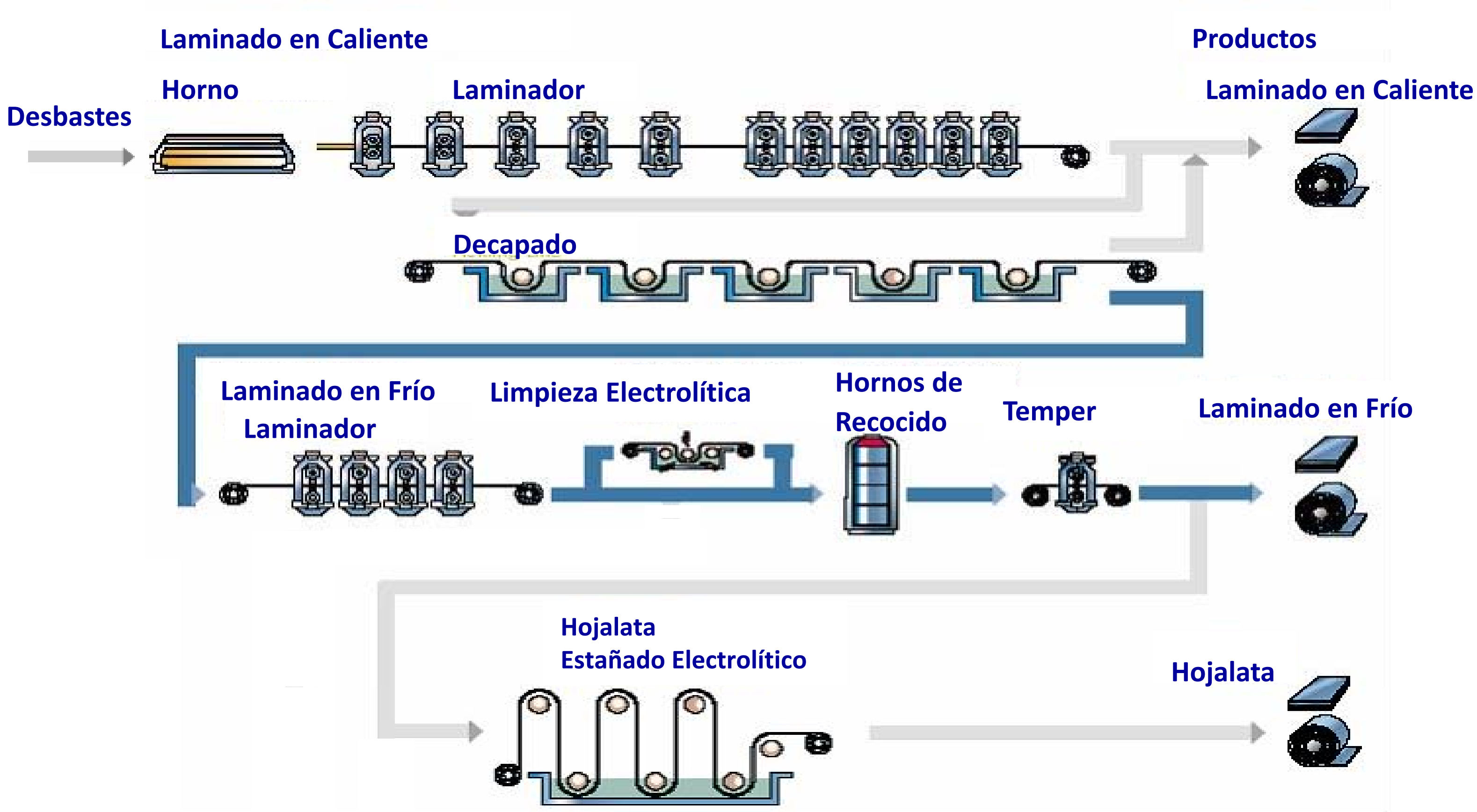

Computational Modeling

- Optimizing production processes
- Developing new products

Modeling of Bulk Metal Forming Processes

- Via the Flow Formulation
- Rigid – viscoplastic material models
- Pseudo-concentrations Technique

Modeling of Bulk Metal Forming Processes

Use Q1-P0 elements (2D) or H1-P0 (3D) elements

or other

non-locking elements to interpolate the velocities and pressures

Perzyna's flow rule - Rigid–Viscoplastic model

$$ {}^{t}s_{\alpha\beta} = 2\,{}^{t}\mu\;{}^{t}d^{VP}_{\alpha\beta} $$

$$ {}^{t}\mu = \frac{\dfrac{{}^{t}\sigma_y}{\sqrt{3}} + \left[\dfrac{\sqrt{3}}{\gamma}\;{}^{t}\dot{\bar{\varepsilon}}_{VP}\right]^{\frac{1}{\delta}}}{\sqrt{3}\;{}^{t}\dot{\bar{\varepsilon}}_{VP}} $$

In the limit, when $\gamma \to \infty$ Eq. (5.168) describes the behavior of a rigid-plastic material (inviscid), in this case,

$$ {}^{t}\mu = \frac{{}^{t}\sigma_y}{3\;{}^{t}\dot{\bar{\varepsilon}}_{VP}}\;. \tag{5.169} $$

The Flow Formulation Via The Pseudo-Concentrations Technique

Eulerian Formulation

In a fixed mesh:

$$c \geqslant 0 \iff \text{there is material at the point,}$$
$$c < 0 \iff \text{there is no material at the point}$$

$\dot{\underline{u}}$: material velocity

$$\begin{aligned} \dot{\underline{u}} \cdot \underline{\nabla} c &= 0 \quad (stationary\ problems) \\ \frac{\partial c}{\partial t} + \dot{\underline{u}} \cdot \underline{\nabla} c &= 0 \quad (transient\ problems) \end{aligned}$$

The Flow Formulation Via The Pseudo-Concentrations Technique

$c>0$	$\mu = \mu_{material}$
$c<0$	$\mu = 10^{\alpha}\ \mu_{material}$ (α = 4 to 6)

Equilibrium Equations via the Augmented Lagrangian Procedure

$$\int_V 2\,\mu^{(k-1)}\,\Delta\dot{\varepsilon}'_{ij}\,\delta\Delta\dot{\varepsilon}'_{ij} dv + \int_V \varkappa\,\Delta\dot{\varepsilon}_v\,\delta\Delta\dot{\varepsilon}_v\,dv =$$

$$\int_V f_i^v\,\delta\Delta\dot{u}_i\,dv\ + \int_{S_\sigma} t_i\,\delta\Delta\dot{u}_i\,dv -$$

$$\int_V s_{ij}^{(k-1)}\,\delta\Delta\dot{\varepsilon}'_{ij} dv - \int_V (p^{(k-1)} + \varkappa\dot{\varepsilon}_v^{(k-1)})\,\delta\Delta\dot{\varepsilon}_v\,dv$$

$$\begin{aligned}
\dot{u}_i^{(k)} &= \dot{u}_i^{(k-1)} + \Delta\dot{u}_i^{(k)} \\
\dot{\varepsilon}_{ij}'^{(k)} &= \dot{\varepsilon}_{ij}'^{(k-1)} + \Delta\dot{\varepsilon}_{ij}'^{(k)} \\
\dot{\varepsilon}_v^{(k)} &= \dot{\varepsilon}_v^{(k-1)} + \Delta\dot{\varepsilon}_v^{(k)} \\
p^{(k)} &= p^{(k-1)} + \varkappa\,\dot{\varepsilon}_v^{(k)}
\end{aligned}$$

Augmented Lagrangian Procedure

Example: Hydrostatic pressure

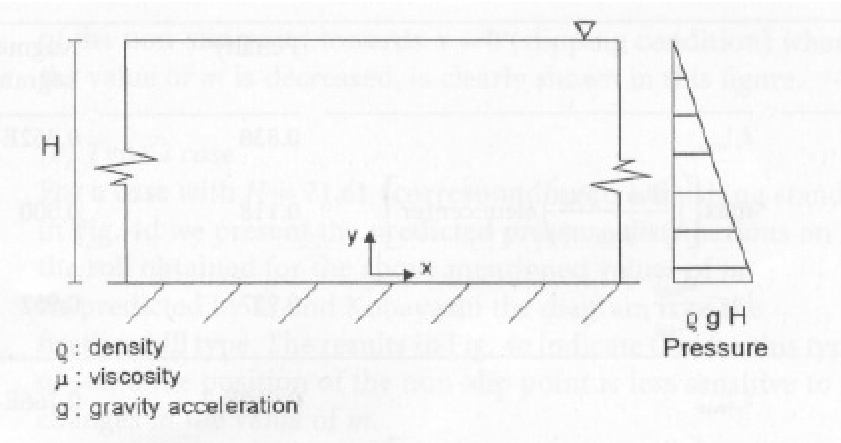

α		Penalty	Augmented Lagrangean
	$\dot{\varepsilon}_v\|_{max}$	0.838	0.362E-8
1	$\max\left[\left(\frac{\|p_{FE}-p_{TH}\|}{p_{TH}}\right)\text{elem.center}\right]$	0.118	0.000
	$\log_{10}\frac{d_{max}}{d_{min}}$	0.957	0.957
	$\dot{\varepsilon}_v\|_{max}$	0.950E-7	0.266E-14
8	$\max\left[\left(\frac{\|p_{FE}-p_{TH}\|}{p_{TH}}\right)\text{elem.center}\right]$	0.000	0.000
	$\log_{10}\frac{d_{max}}{d_{min}}$	7.335	7.335

d_i: diagonal element of the factorized stiffness matrix
p_{TH}: theoretical pressure
p_{FE}: finite element predicted pressure

Augmented Lagrangian Procedure

Example: Extrusion

Table 2. Extrusion case

α	$\log_{10} \frac{d_{max}}{d_{min}}$
1	4.67
8	11.43

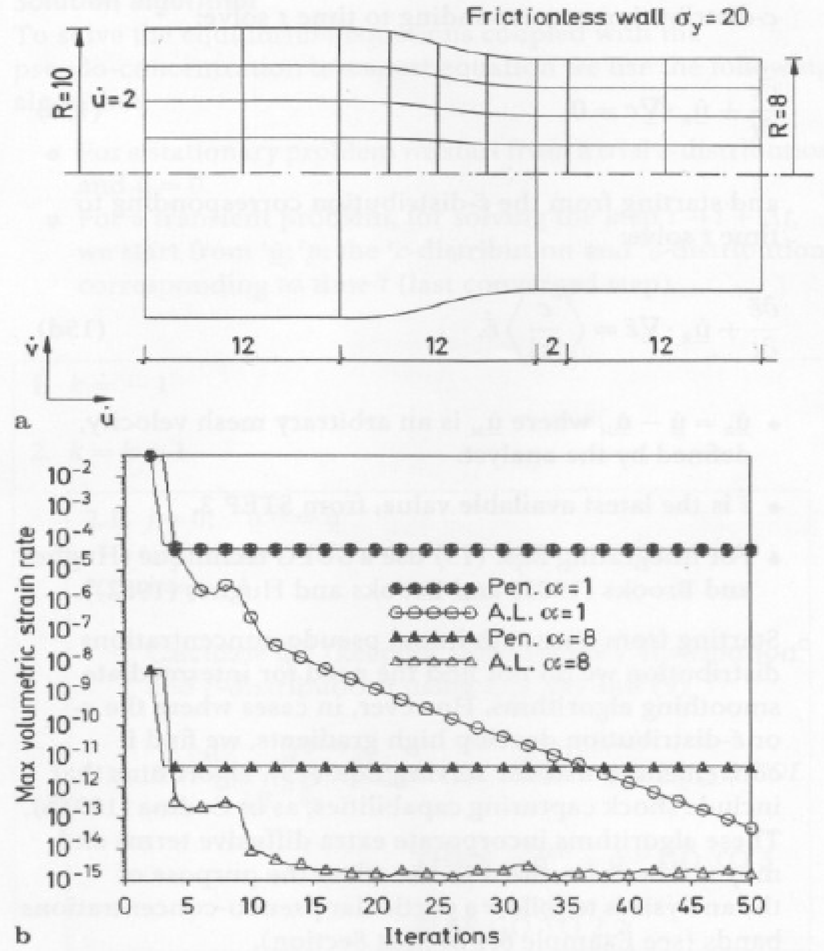

Transport Equations for the Equivalent Plastic Strain

$\dot{\bar{\varepsilon}}$: material derivative of the equivalent plastic strain.

$$\dot{\bar{\varepsilon}} = \left(\frac{2}{3} \dot{\varepsilon}_{ij} \dot{\varepsilon}_{ij} \right)^{\frac{1}{2}}$$

$$\dot{\bar{\varepsilon}} = \frac{D\,\bar{\varepsilon}}{D\,t} = \frac{\partial \bar{\varepsilon}}{\partial t} + \underline{\dot{u}} \cdot \underline{\nabla} \bar{\varepsilon}$$

$$\underline{\dot{u}} \cdot \underline{\nabla} \bar{\varepsilon} = \frac{\langle c \rangle}{|c|} \dot{\bar{\varepsilon}} \quad (stationary\ problems)$$

$$\frac{\partial \bar{\varepsilon}}{\partial t} + \underline{\dot{u}} \cdot \underline{\nabla} \bar{\varepsilon} = \frac{\langle c \rangle}{|c|} \dot{\bar{\varepsilon}} \quad (transient\ problems)$$

c-dependent Boundary Conditions

For nodes that are in contact with forming tools:

$$
\begin{aligned}
c &< 0 \Longrightarrow \dot{u}_n = free \\
c &\geqslant 0 \Longrightarrow \dot{u}_n = 0
\end{aligned}
$$

At the contact nodes we impose friction:

- Coulomb friction law
- Constant friction law

C-dependent Boundary Conditions

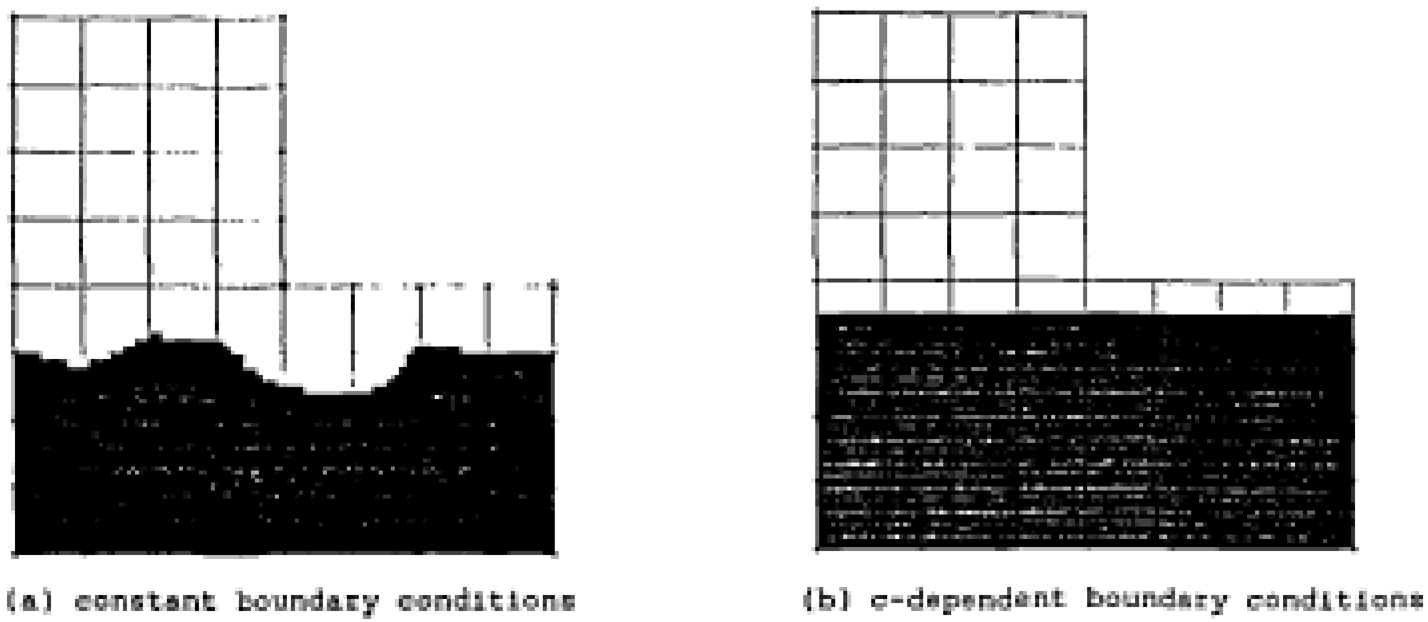

Figure 1 Artificial bubbles in a mould filling problem

Solution Algorithm

1. $k = -1$

2. $k = k + 1$

   2.1. $j = 0; \quad \dot{\underline{\mathbf{u}}}^{(j)} = \dot{\underline{\mathbf{u}}}^{(k-1)}$

   2.2. $j = j + 1$

   Calculate $\dot{\underline{\mathbf{u}}}^{(j)}$ (keeping constant the c-distribution and $\bar{\varepsilon}$-distribution) using Eqs. (8) and (9)

   2.3. IF $\dfrac{\| \dot{\underline{\mathbf{u}}}^{(j)} - \dot{\underline{\mathbf{u}}}^{(j-1)} \|_2}{\| \dot{\underline{\mathbf{u}}}^{(j)} \|_2} \leq UTOL$ and $\| \dot{\varepsilon}_v^{(j)} \|_\infty \leq VTOL$

   THEN $\rightarrow \dot{\underline{\mathbf{u}}}^{(k)} = \dot{\underline{\mathbf{u}}}^{(j)}$ GO TO 3

   ELSE GO TO 2.2

3. Calculate the c-distribution and $\bar{\varepsilon}$-distribution using Eq. (15)

4. IF $k = 0$ GO TO 2

5. IF $\dfrac{\| \dot{\underline{\mathbf{u}}}^{(k)} - \dot{\underline{\mathbf{u}}}^{(k-1)} \|_2}{\| \dot{\underline{\mathbf{u}}}^{(k)} \|_2} \leq UTOL$ and $\| \dot{\varepsilon}_v^{(k)} \|_\infty \leq VTOL$

   THEN $\rightarrow$ convergence

   ELSE GO TO 2

Solution Algorithm

$$\int_V 2\mu\Delta\dot{\varepsilon}'_{ij}\delta\Delta\dot{\varepsilon}'_{ij}dv + \int_V \kappa\Delta\dot{\varepsilon}_v\delta\Delta\dot{\varepsilon}_v dv = \int_V f_i^v\delta\Delta\dot{u}_i dv + \int_{S_\sigma} t_i^*\delta\Delta\dot{u}_i ds$$

$$- \int_V s_{ij}^{(k-1)}\delta\Delta\dot{\varepsilon}'_{ij}dv$$

$$- \int_V (p^{(k-1)} + \kappa\dot{\varepsilon}_v^{(k-1)})\,\delta\Delta\dot{\varepsilon}_v dv \tag{8}$$

κ: penalty parameter.

Then we update,

$$\dot{u}_i^{(k)} = \dot{u}_i^{(k-1)} + \Delta\dot{u}_i; \quad \dot{\varepsilon}'^{(k)}_{ij} = \dot{\varepsilon}'^{(k-1)}_{ij} + \Delta\dot{\varepsilon}'_{ij}$$

$$\dot{\varepsilon}_v^{(k)} = \dot{\varepsilon}_v^{(k-1)} + \Delta\dot{\varepsilon}_v; \quad p^{(k)} = p^{(k-1)} + \kappa\dot{\varepsilon}_v^{(k)}. \tag{9}$$

Solution Algorithm

$$\underline{\dot{u}} \cdot \underline{\nabla} c = 0 \tag{15a}$$

$$\underline{\dot{u}} \cdot \underline{\nabla}\bar{\varepsilon} = \left\langle \frac{c}{|c|} \right\rangle \dot{\bar{\varepsilon}}. \tag{15b}$$

In STEP 3 for transient problems, starting from the c-distribution corresponding to time t solve:

$$\frac{\partial c}{\partial t} + \underline{\dot{u}}_R \cdot \underline{\nabla} c = 0 \tag{15c}$$

and starting from the $\bar{\varepsilon}$-distribution corresponding to time t solve:

$$\frac{\partial \bar{\varepsilon}}{\partial t} + \underline{\dot{u}}_R \cdot \underline{\nabla}\bar{\varepsilon} = \left\langle \frac{c}{|c|} \right\rangle \dot{\bar{\varepsilon}}. \tag{15d}$$

Stationary Case

Rolling of Steel Plates

$$H = \frac{R}{t_{in}}\left[\frac{t_{in} - t_{out}}{t_{in}}\right]$$

$H < 3$ indicates a double peaks type contact pressure distribution. In this case the deformation pattern is more inhomogeneous (type 1)

Type 1

$H > 3$ indicates a friction-hill type contact pressure distribution. In this case the deformation pattern is more homogeneous (type 2)

Type 2

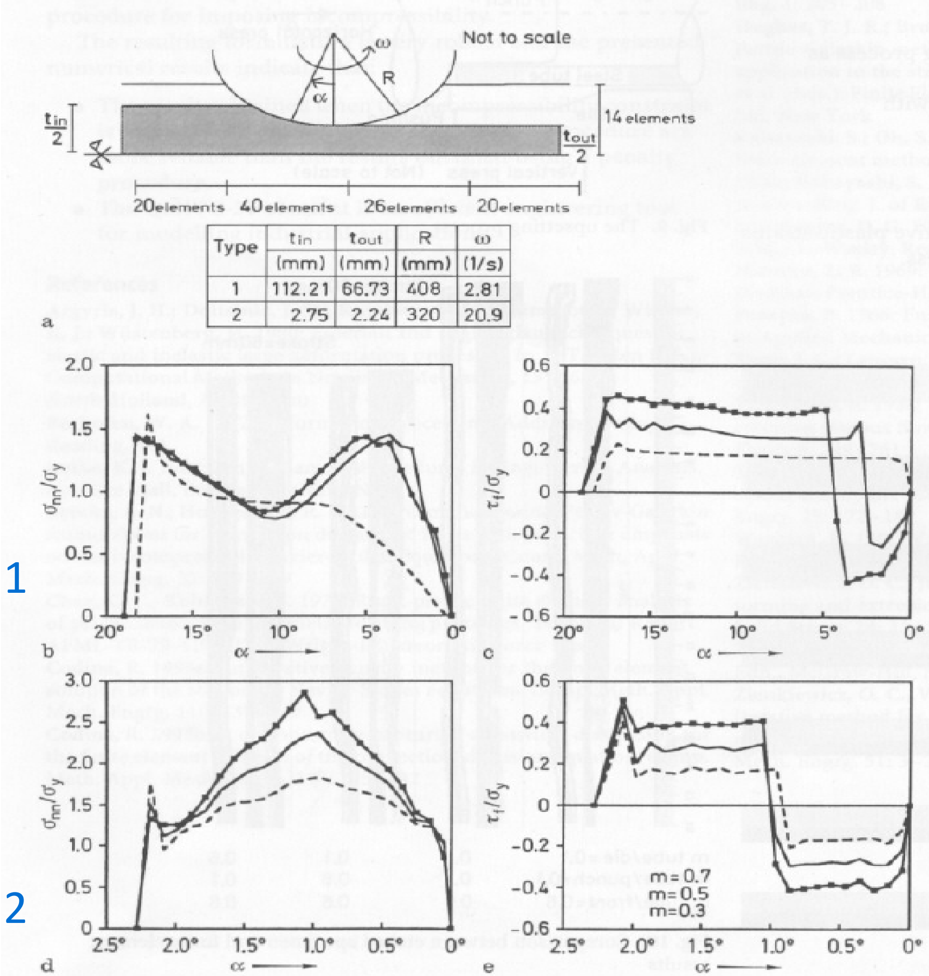

Type	t_{in} (mm)	t_{out} (mm)	R (mm)	ω (1/s)
1	112.21	66.73	408	2.81
2	2.75	2.24	320	20.9

Transient Case

Upsetting process

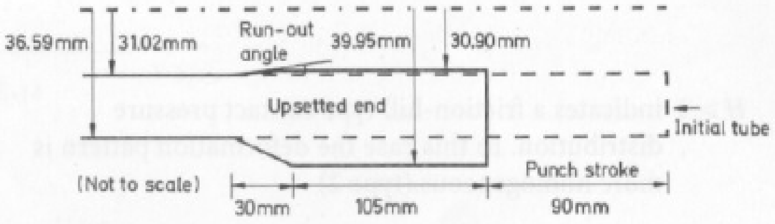

Fig. 8. Upsetted end of a steel tube

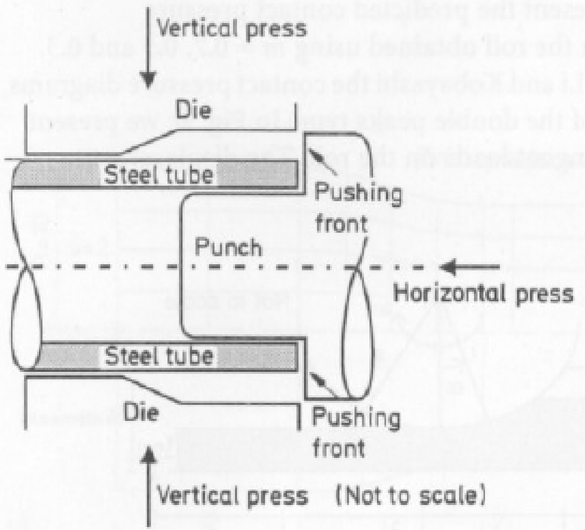

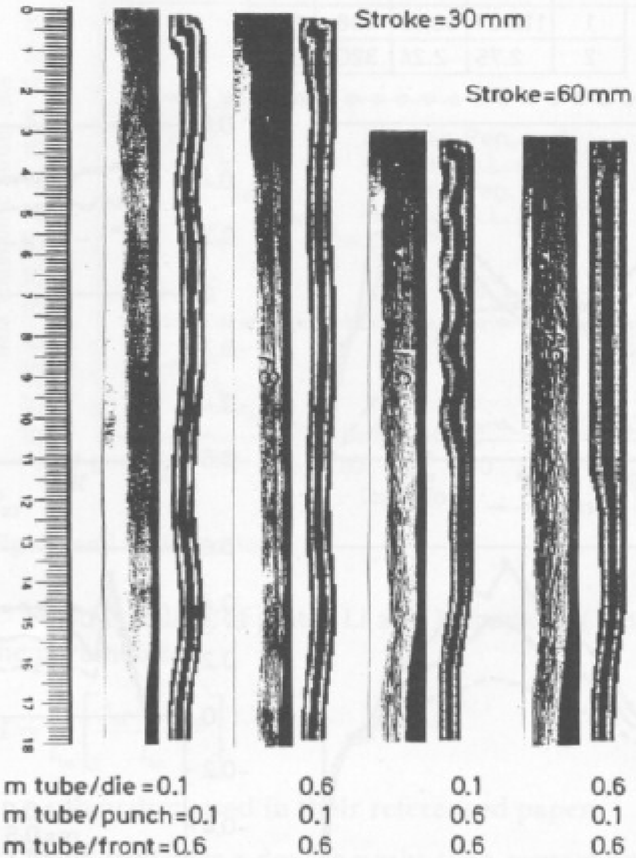

Fig. 10. Comparison between etched specimen and finite element results

Thermo – Mechanical Coupling

Equilibrium equations

$$\overline{\sigma} = \sigma_y = \sigma_y(\overline{\varepsilon}, \dot{\overline{\varepsilon}}, T)$$

Heat transfer equations

In domain W

$$\rho\, C\, \dot{T} = \underline{\nabla} \cdot k\, \underline{\nabla} T + \beta\, \underline{\underline{\sigma}} : \underline{\underline{\dot{\epsilon}}}^p$$

ß: Taylor-Quinney coefficient (between 0.85 and 0.95)

In contour G_n=G - G_T

$$q_n = -k\, \underline{\nabla} T \cdot \underline{n}$$ Heat flux boundary condition

Experimental Model Validation

Gleeble 3500 Simulator
CINI (Tenaris)

Experimental Model Validation

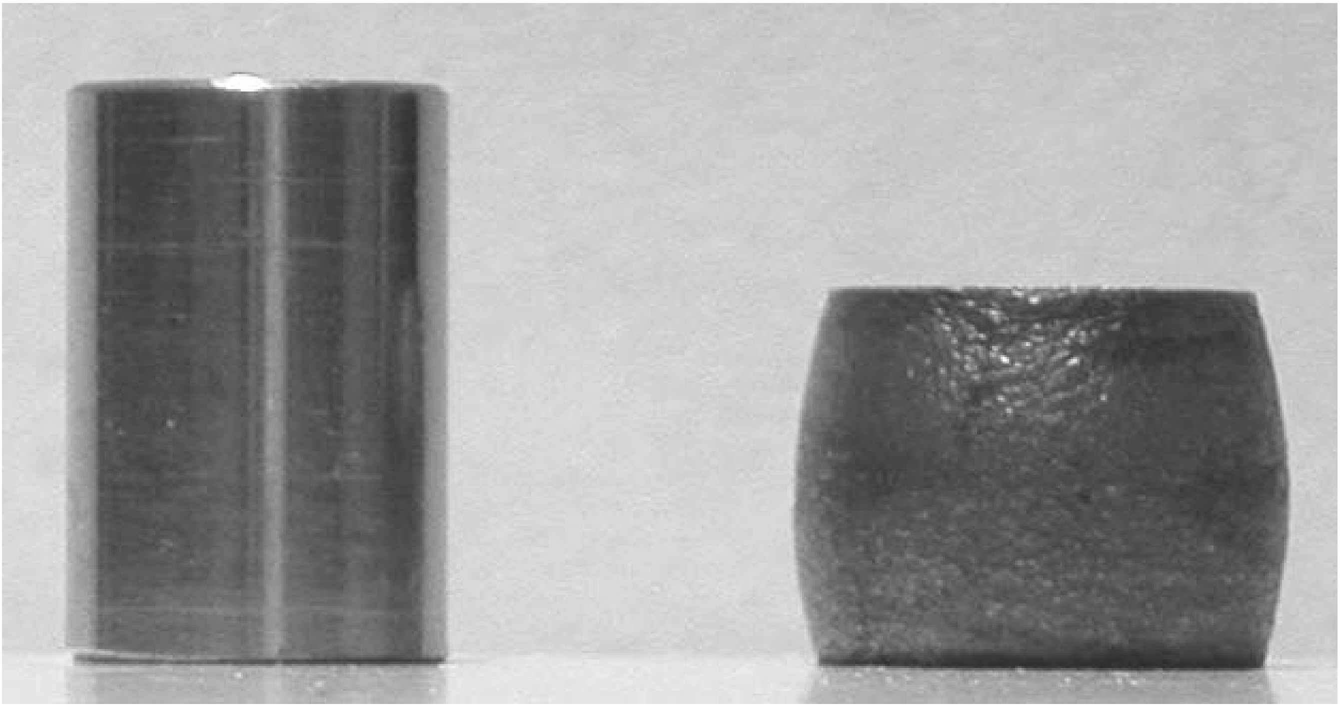

Undeformed sample

Deformed sample

Experimental Model Validation

Temperature prediction validation

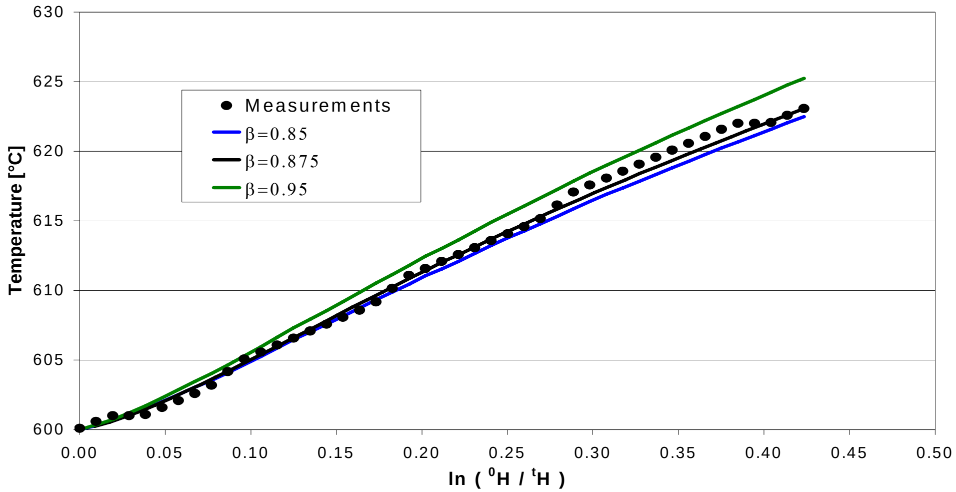

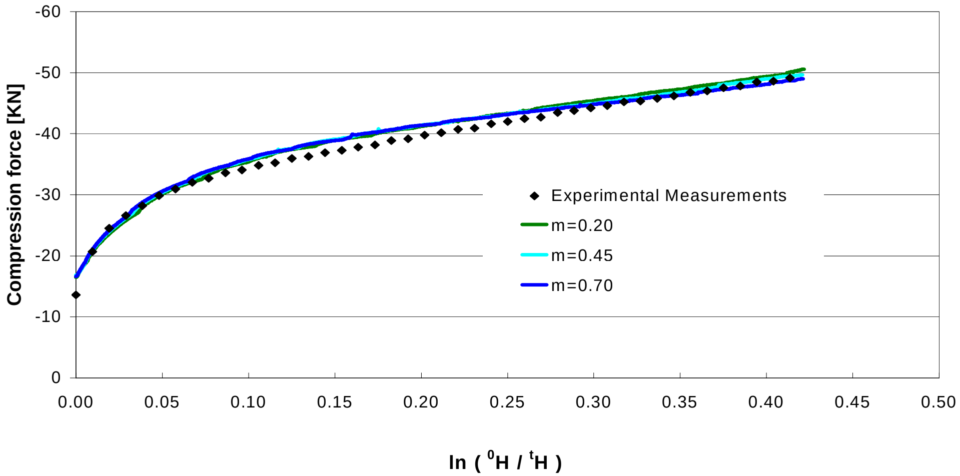

Compresion force prediction validation

Experimental Model Validation

Barreling

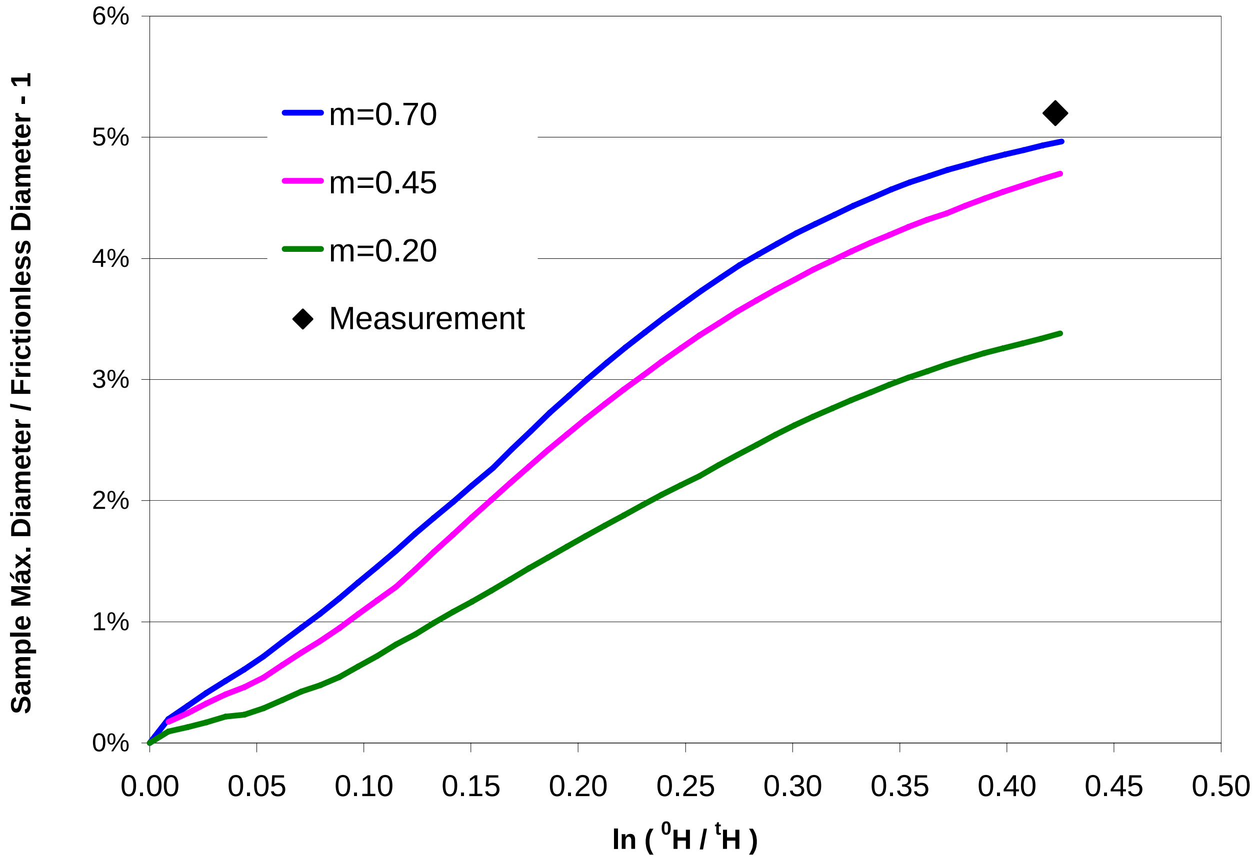

Hot Rolling of Steel Coils

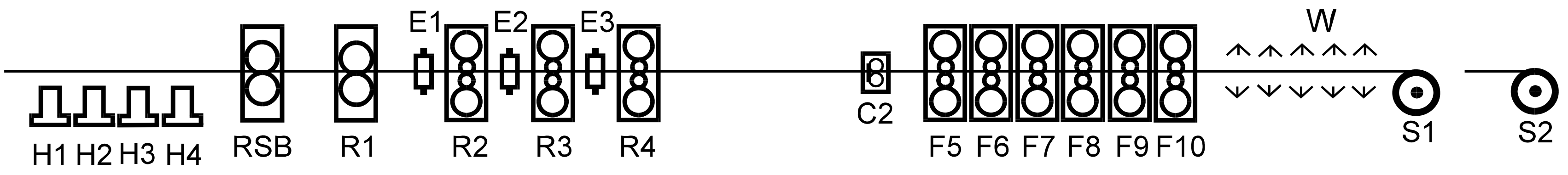

RSB : roughing scale breaker
R1, R2, R3, R4 : roughing stands
E1, E2, E3 : edger rolls
H1, H2, H3, H4 : re-heating furnaces

C2 : crop shear
F5, F6, F7, F8, F9, F10 : finishing stands
W : water cooling
S1, S2 : sheet coilers

Figure 3: Hot rolling mill

3D Modeling of Hot Rolling

Couple:

- Eulerian formulation that describes the rolled steel deformation
- Standard Lagrangian formulation that describes the rolls deformation

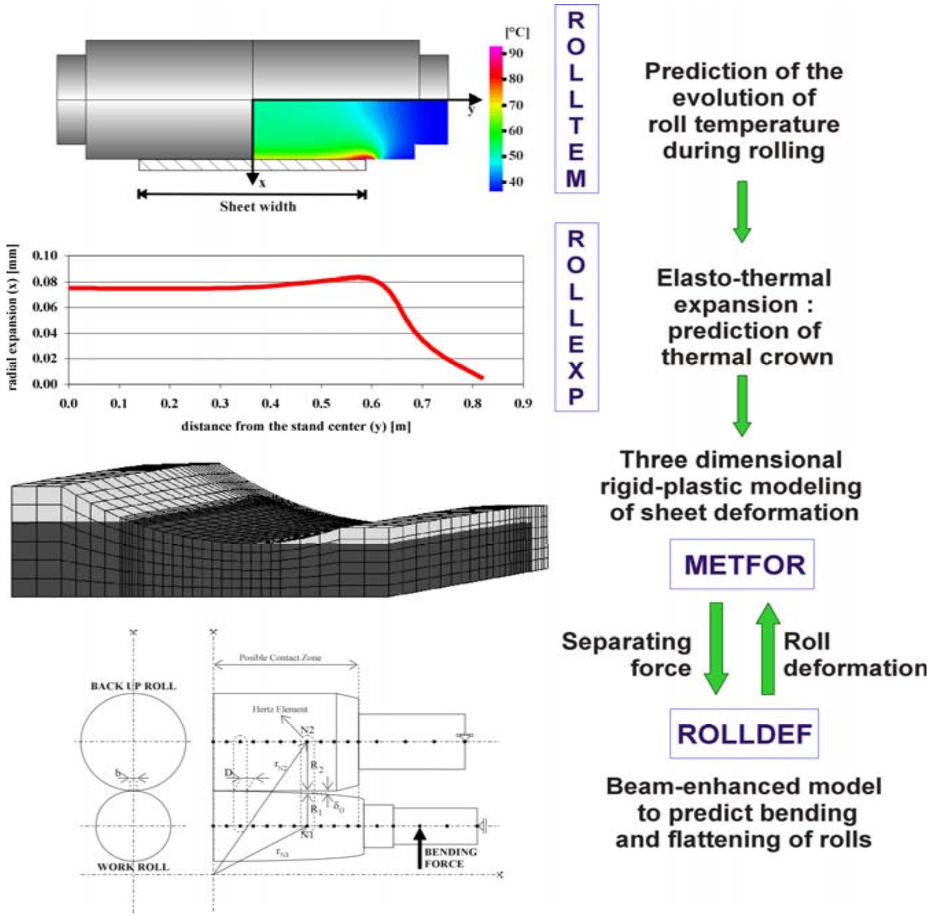

Phenomenological Constitutive Relations

Material properties

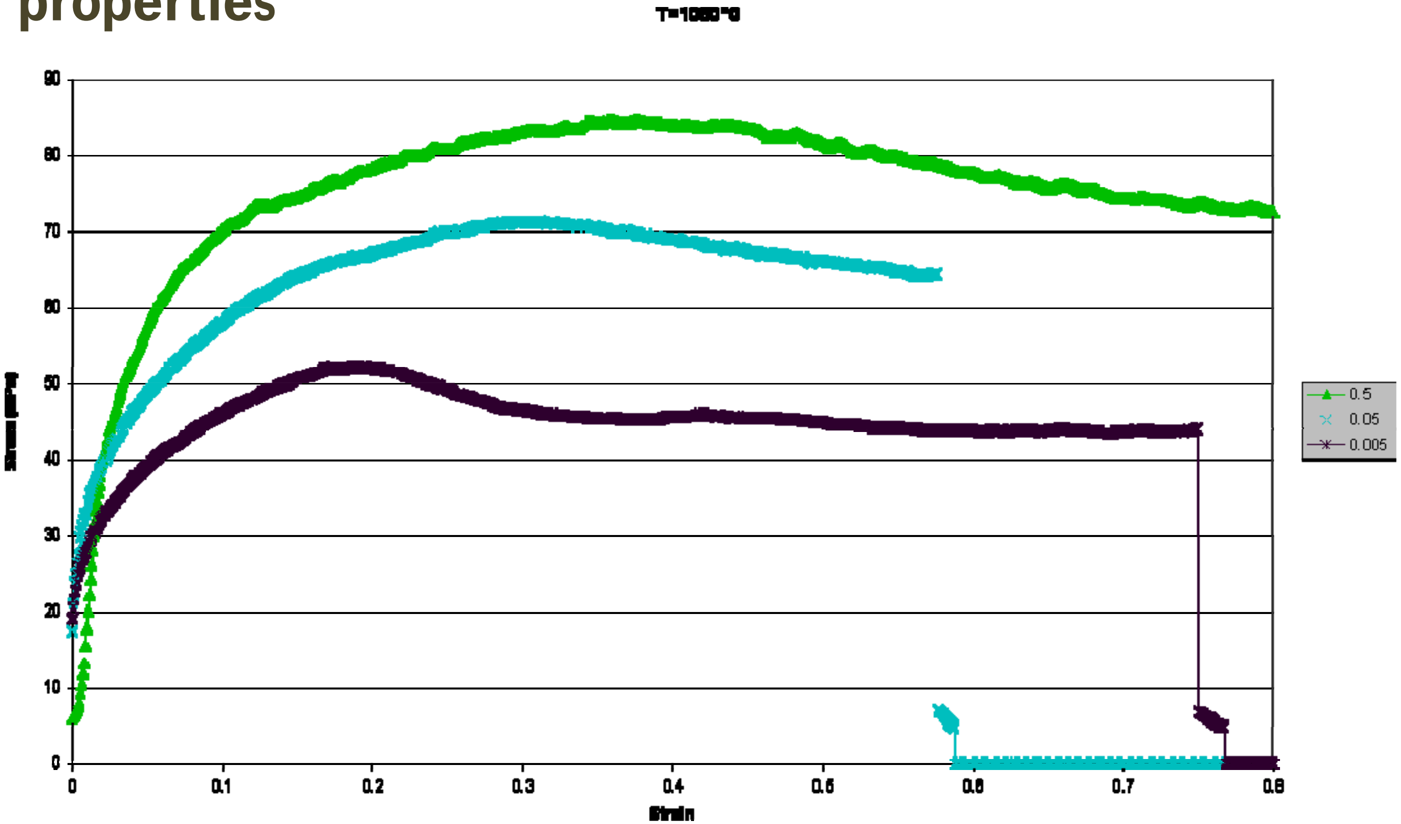

Compression tests at elevated temperature showing recristallization

Modeling of bulk metal – forming processes

Phenomenological constitutive equations

1. The Fields – Backofen law

$$\sigma_y = A(T)\, \bar{\varepsilon}^{n(T)}\, \dot{\bar{\varepsilon}}^{m(T)}$$

This model cannot represent recristalization phenomena

2. Exponential – power law 1

$$\sigma_y = [A(T)\, e^{-B(T)\bar{\varepsilon}}\, (\bar{\varepsilon} + \bar{\varepsilon}_o)^{n(T)} + C(T)\, (1 - e^{-B(T)\bar{\varepsilon}})]\, \dot{\bar{\varepsilon}}^{m(T)}$$

3. Exponential – power law 2

$$\sigma_y = [A(T)\, e^{-B(T)\bar{\varepsilon}}\, \sqrt{(1 - e^{-n(T)(\bar{\varepsilon}+\bar{\varepsilon}_o)})} + C(T)\, (1 - e^{-B(T)\bar{\varepsilon}})]\dot{\bar{\varepsilon}}^{m(T)}$$

Modeling of bulk metal – forming processes

Mechanical tests to determine the material constants

- Tension tests. Strain limitations
- Compression tests logarithmic strain < 0.8

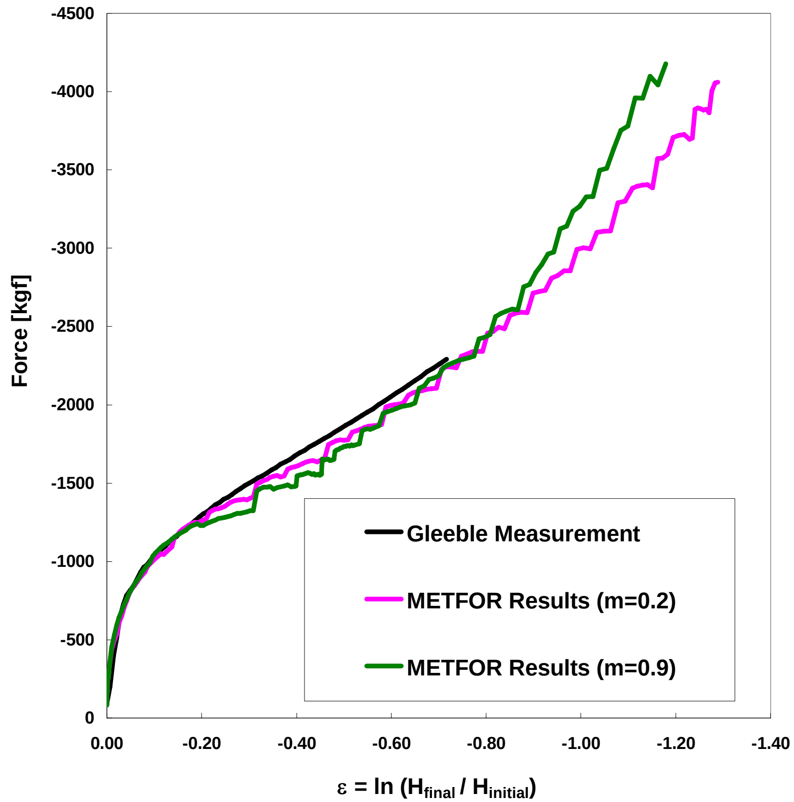

Samples barreling

Samples final shape

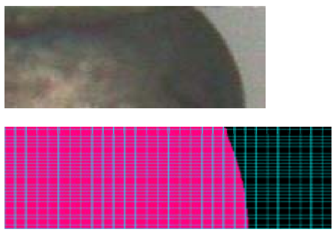

FEM
Light friction; m=0.2

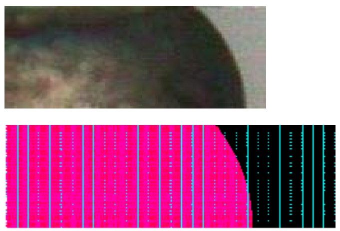

FEM
Hight friction; m=0.9

Modeling of bulk metal – forming processes

Compression tests

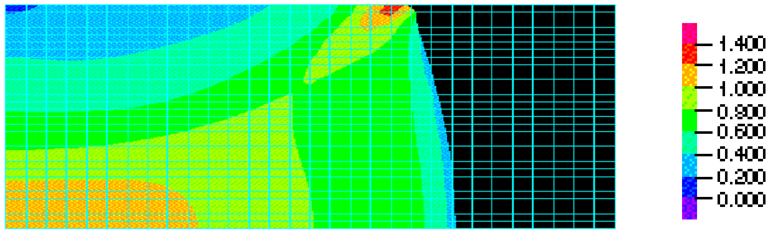

m=0.2

Coeficiente de fricción m= 0.2

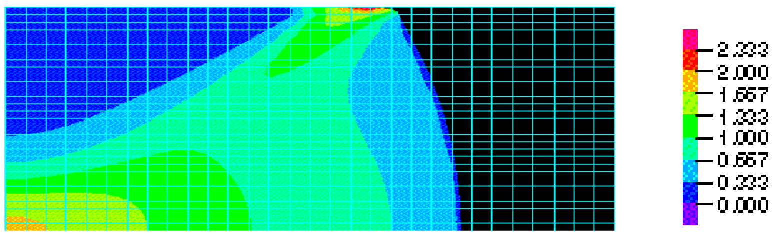

m=0.9

Coeficiente de fricción m= 0.9

When there is friction, it fails to represent a uniform strain test

Modeling of bulk metal – forming processes

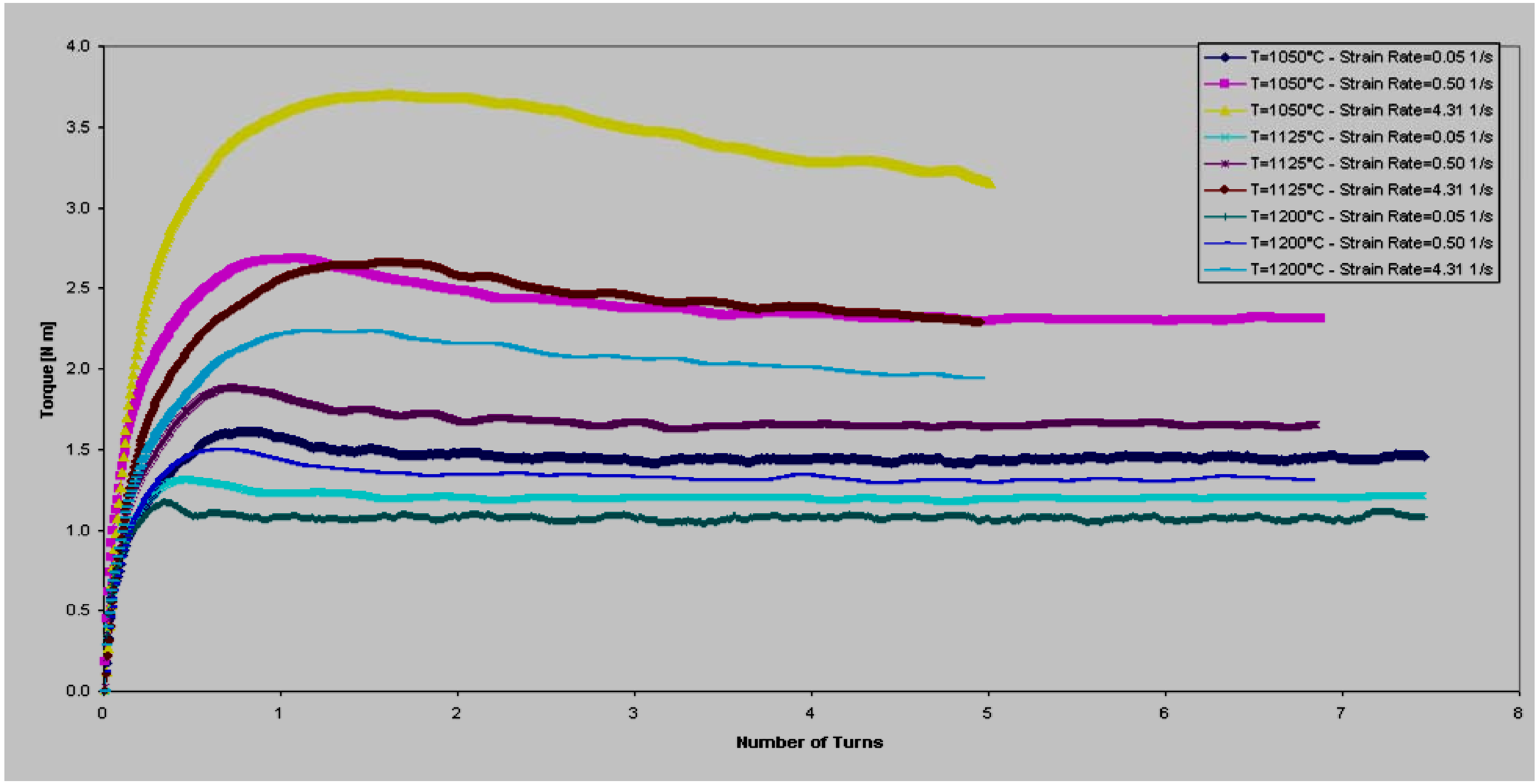

The torsion test

Modeling of bulk metal – forming processes

Results obtained using TESTPOST

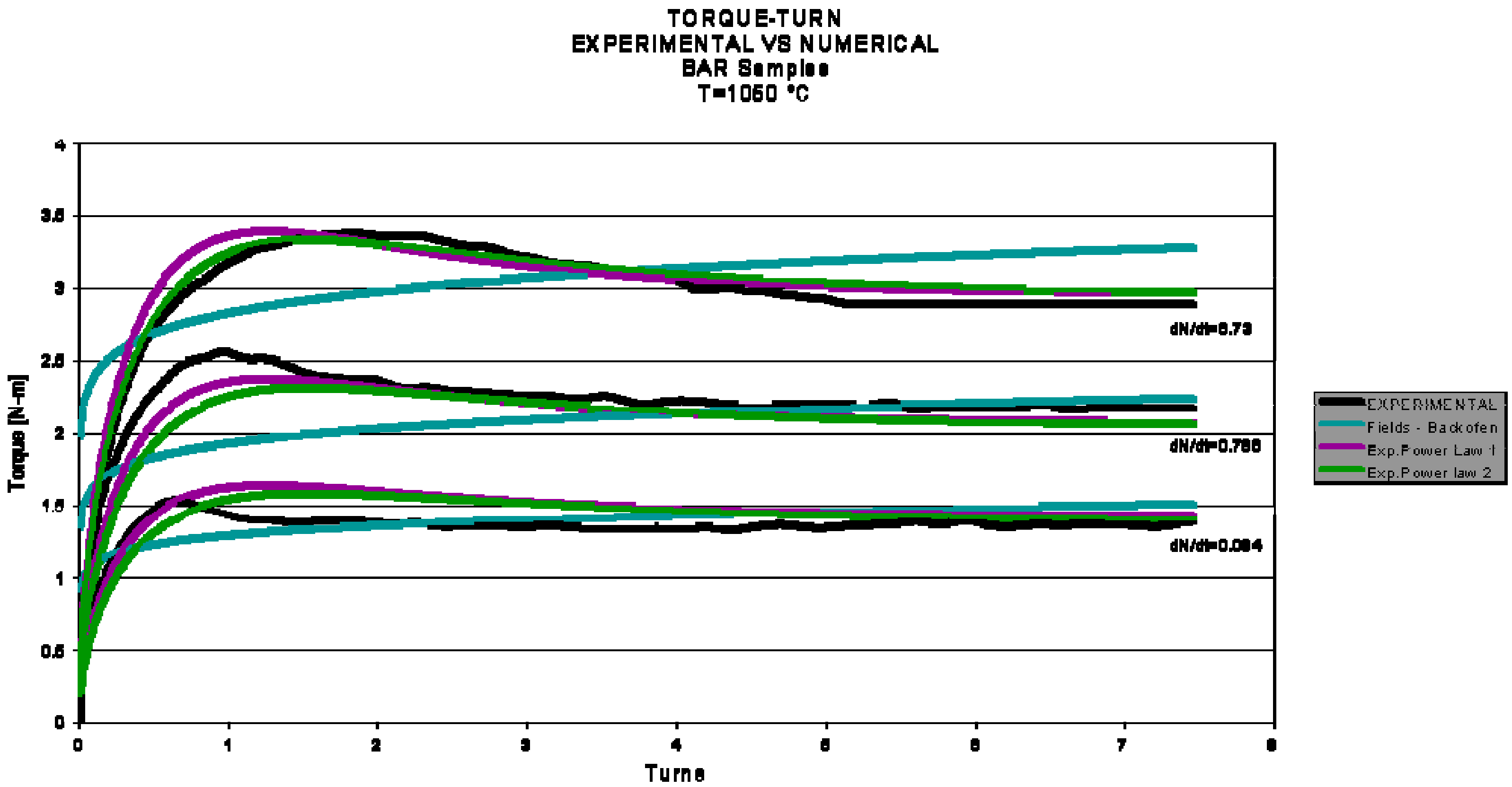

Hot Rolling of Steel Plates

Model validation at the F10

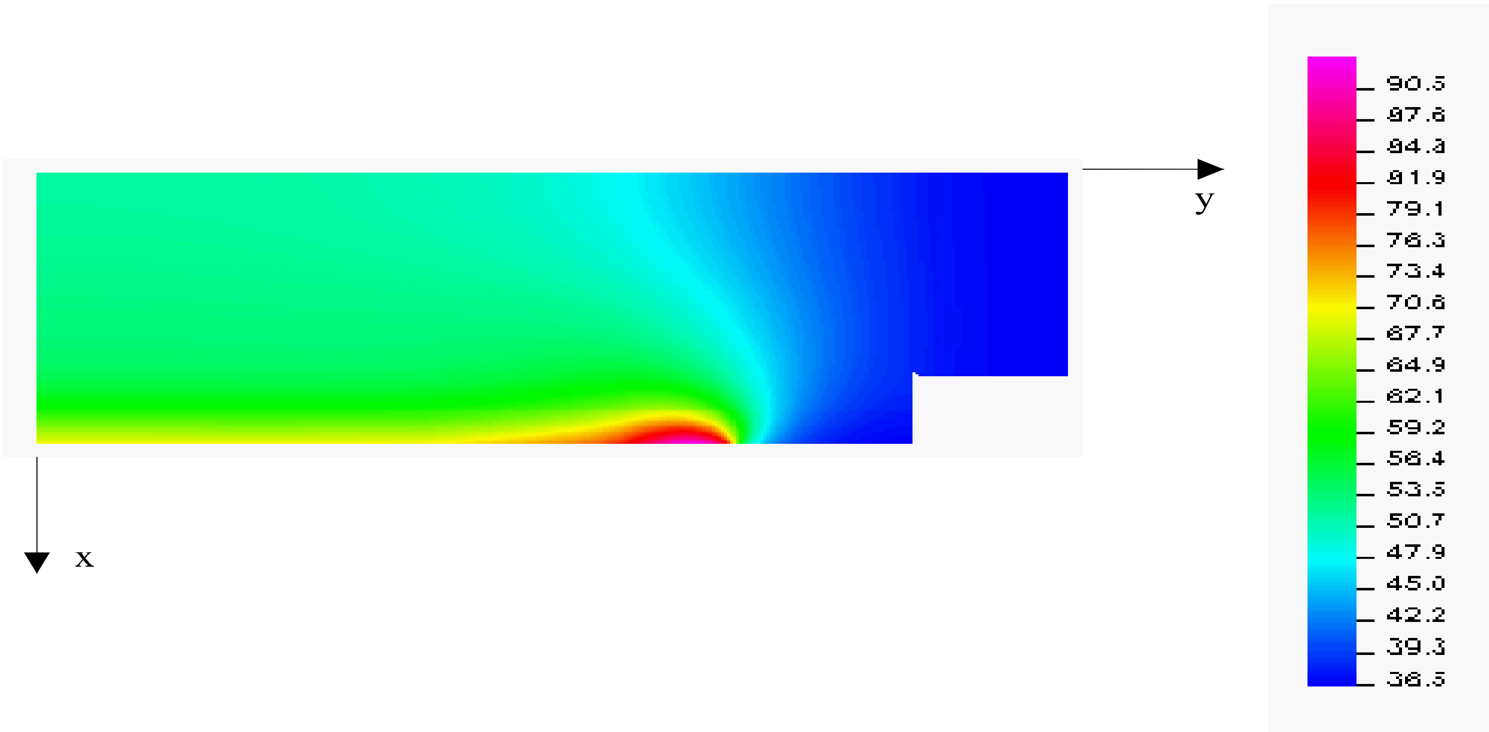

Temperature map of the work roll at the instant at which the last coil exits the stand F10 (t_{out})

Hot Rolling of Steel Plates

Model validation at the F10

Stand F10				
Coil N°	Width [mm]	Time In [sec]	Time Out [sec]	
1	1046	0	60	
2	1040	155	215	
3	1042	286	345	
4	1045	373	432	
5	1044	469	531	
6	1041	567	624	
7	1146	653	713	
8	1143	753	813	
9	1257	856	915	
10	1260	962	1021	
11	1262	1077	1136	
12	1263	1205	1264	
13	1264	1309	1368	
14	1262	1415	1474	
Time of the interruption of the refrigerating water				1535 sec
Begining of the measurement of roll surface temperature				1795 sec
Ending of the measurement of roll surface temperature				1975 sec

Finite element simulation of work roll temperature build-up

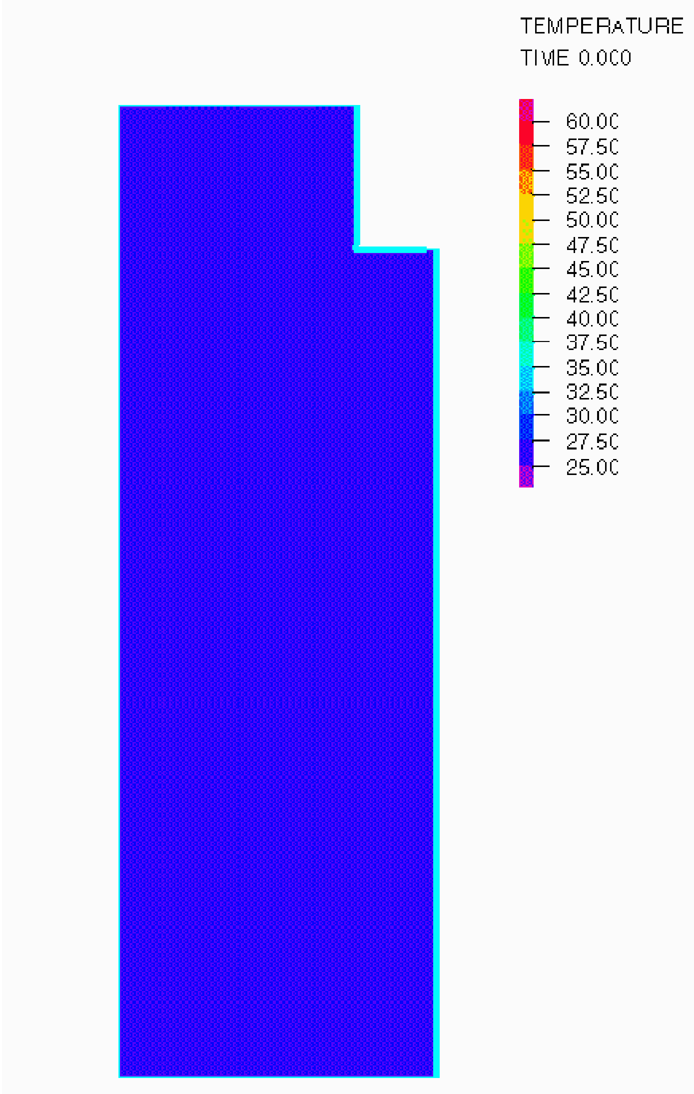

Hot Rolling of Steel Plates

Model validation at the F10

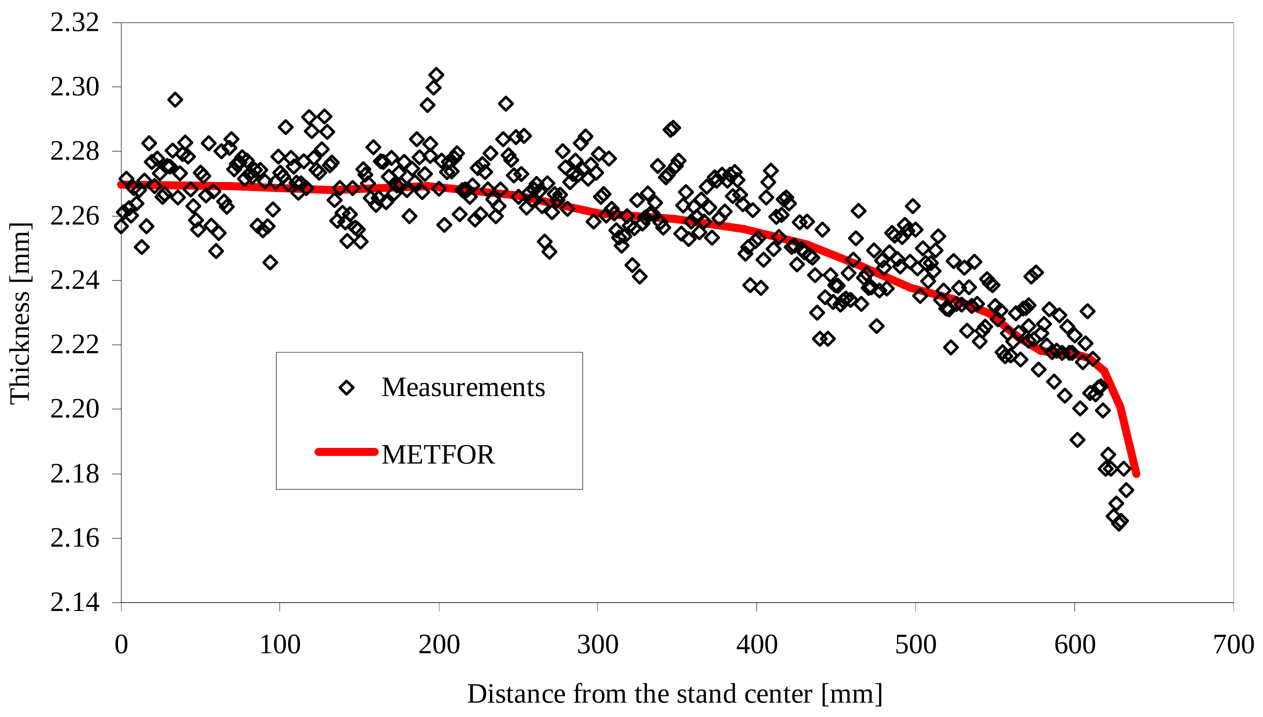

Asymmetric Rolling

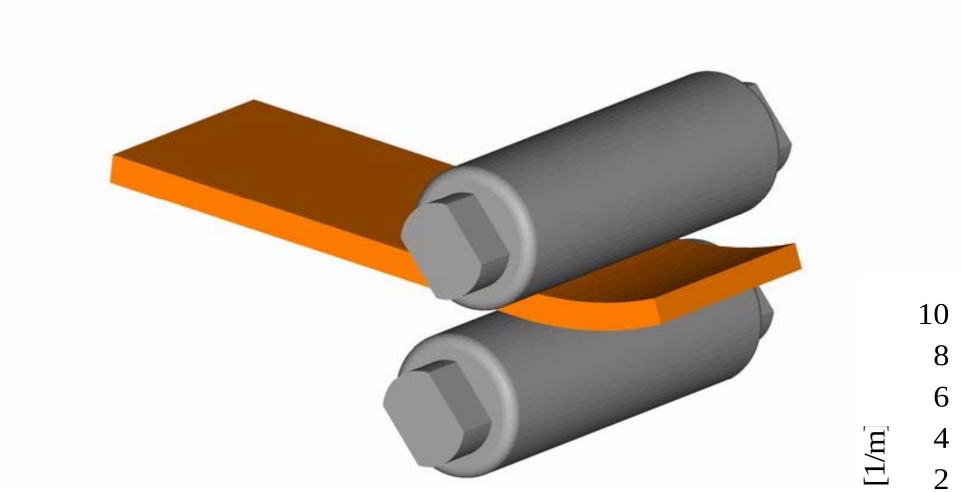

$\phi_{upper\ roll}$ = 184 mm
$\phi_{lower\ roll}$ = 202 mm

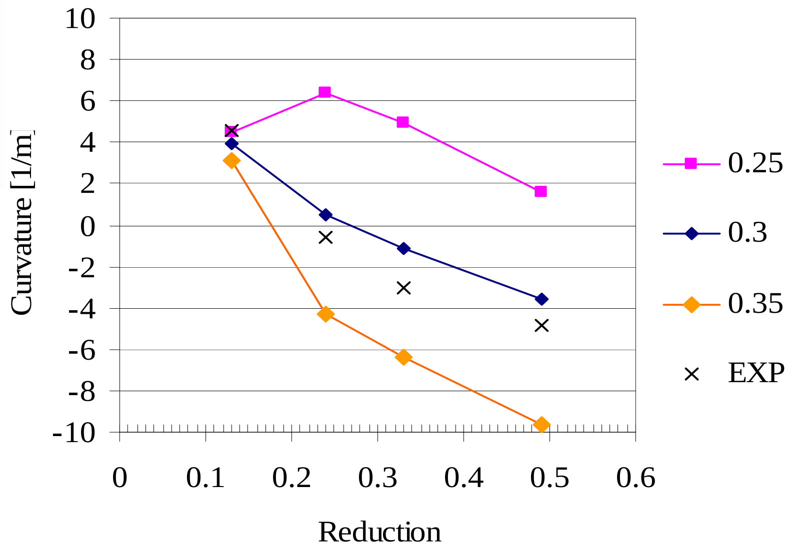

Experimental (aluminum) results and FEM results for various “m”

Vertical Rolling (edging)

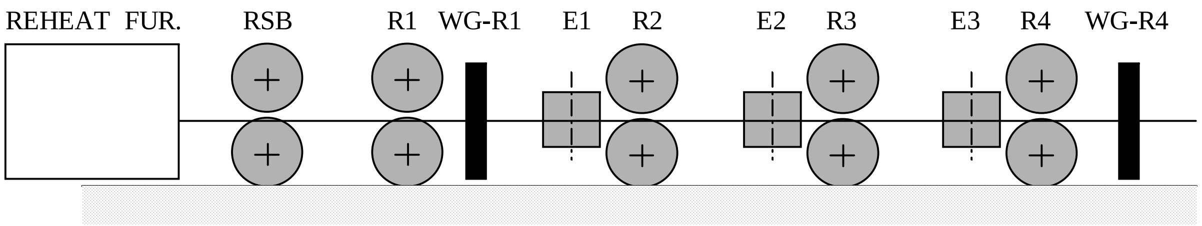

Vertical Rolling (edging)

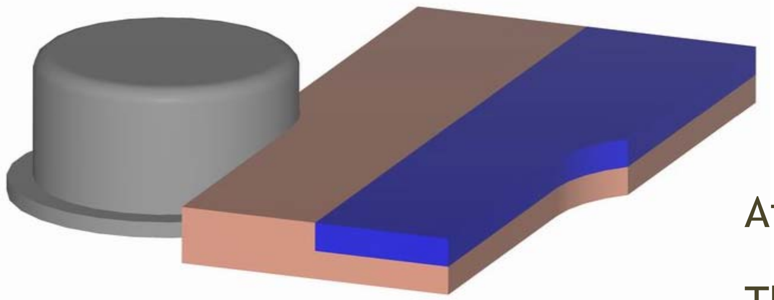

After edging

The dog bone

Before edging

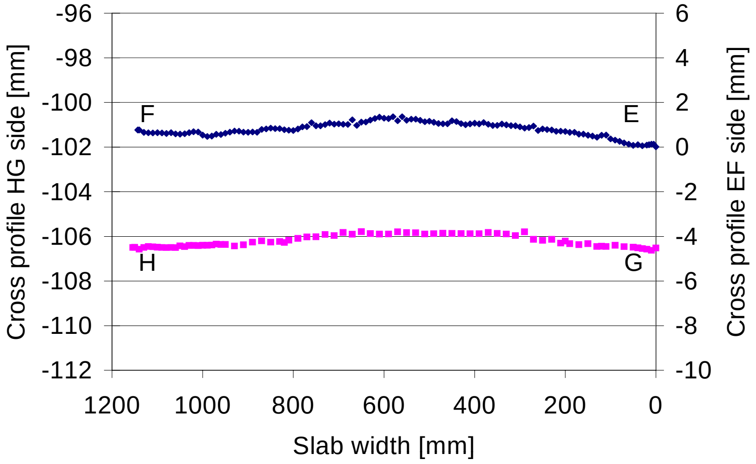

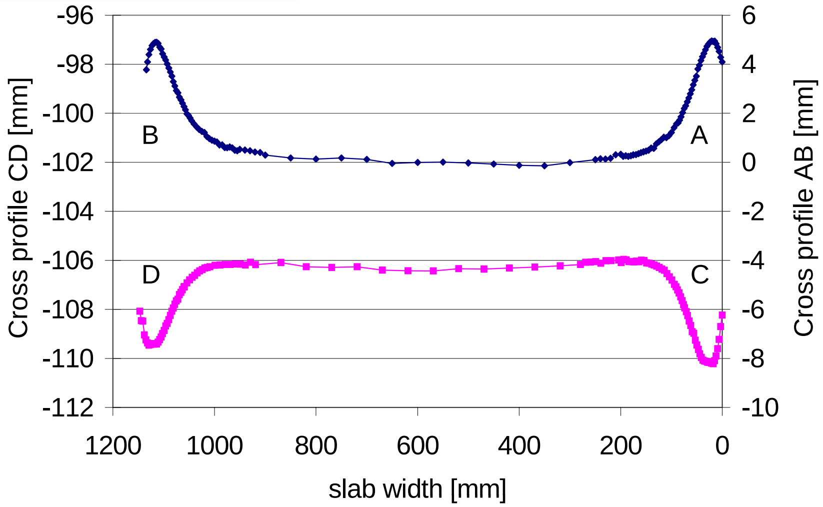

Vertical Rolling (edging)

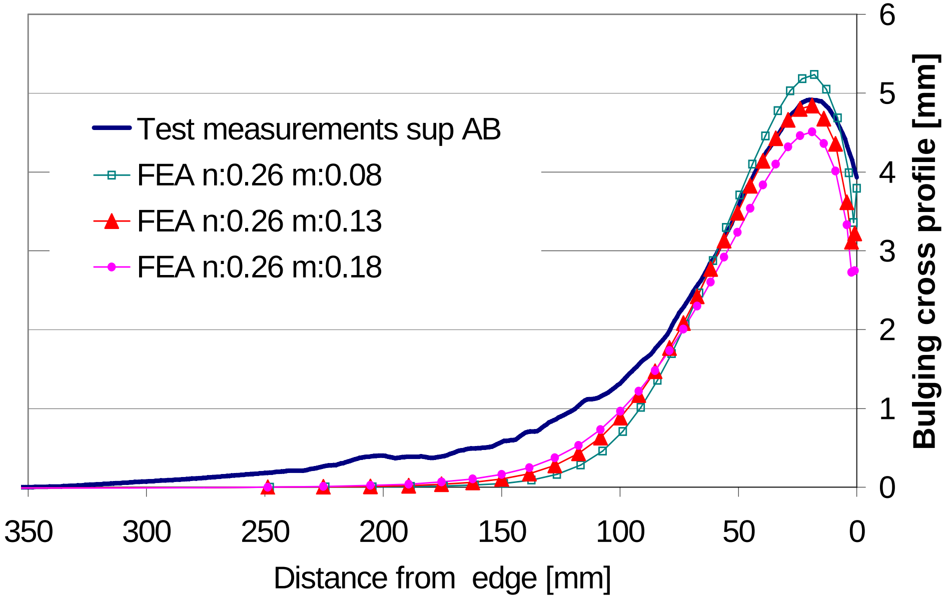

Experimental validation of numerical results

Product Process Steel Seamless Pipes

The Mannesmann piercing process

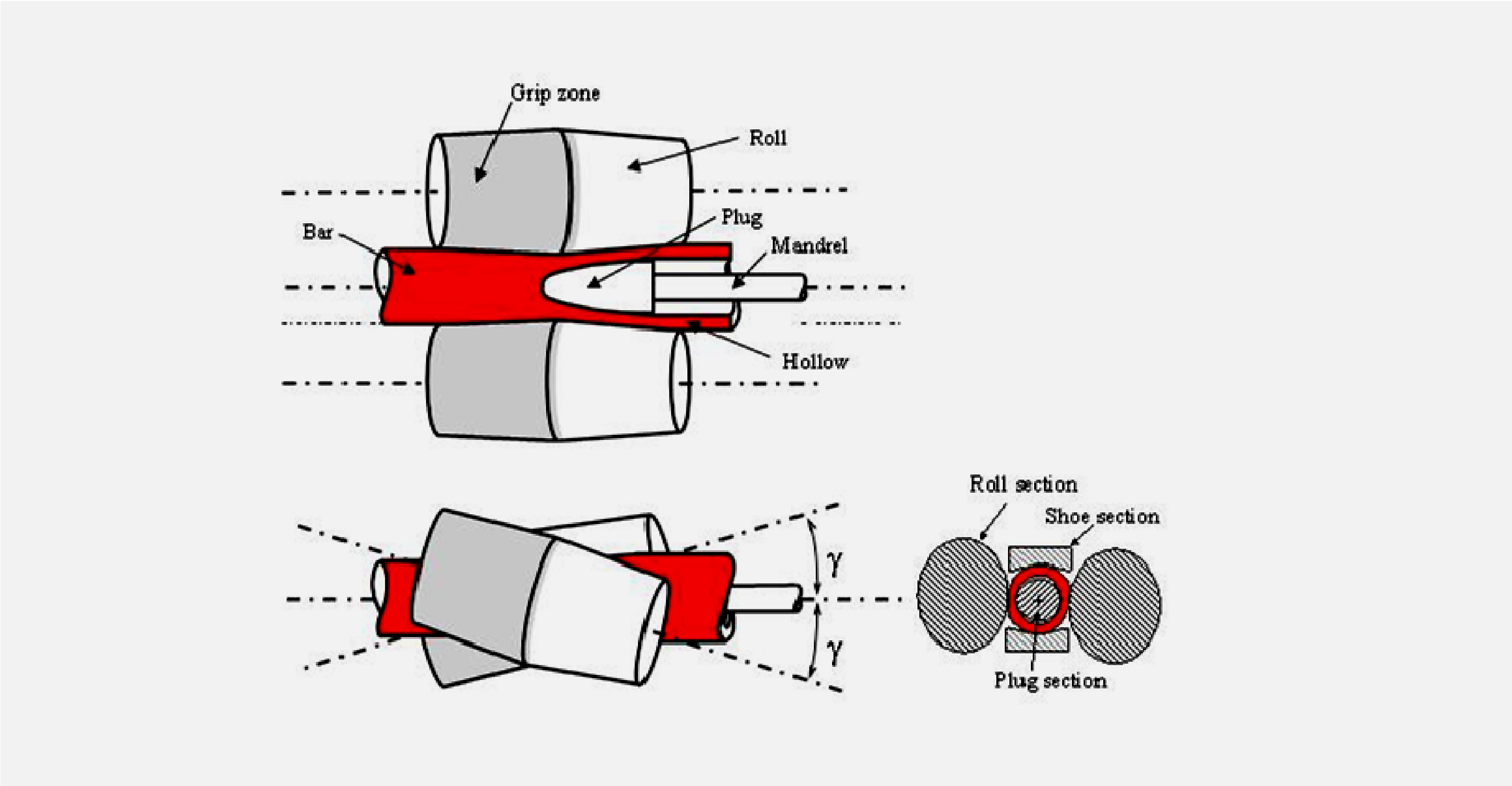

Model Validation

	Profile scheme	Bar diameter
Case 1		395 mm
Case 2		395 mm
Case 3	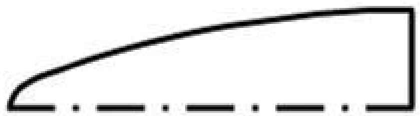	215 mm

Model Validation

Plug #	# Elements	# d.o.f.	FEM-helix pitch	Exp.-helix pitch
1	96,576	309,547	1158 mm	1054 mm
2	100,950	322,894	714 mm	695 mm

Model Validation

Plug # 1
(interrupted piercing)

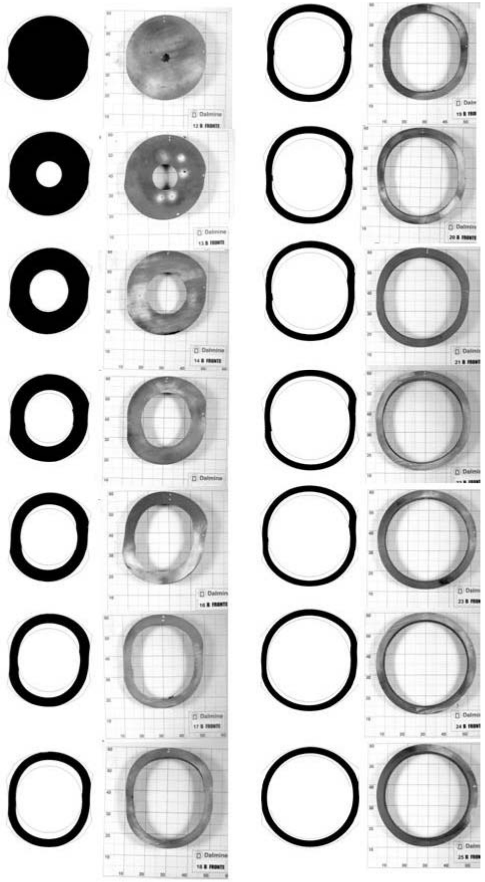

SIM&TEC Simulación y Tecnología Simulation and Technology

Model Validation

Sensitivity analyses

Plug	μ_{rolls}	μ_{shoes}	μ_{plug}	$L_{Mann.}$	FEM-pitch	$\frac{FEM\ \text{pitch}}{Exp.\text{pitch}}$
1	0.2	0.2	0.35	λ_1	1054 mm	0.88
1	0.5	0.2	0.35	λ_1	1252 mm	1.05
1	0.2	0.2	0.35	$2\lambda_1$	1158 mm	0.97
2	0.2	0.2	0.35	λ_2	695 mm	0.88
2	0.5	0.2	0.35	λ_2	899 mm	1.14
2	0.2	0.2	0.35	$2\lambda_2$	714 mm	0.90

Model Validation

Mapping of the inner and outer surfaces (interrupted piercing)



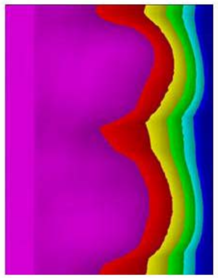

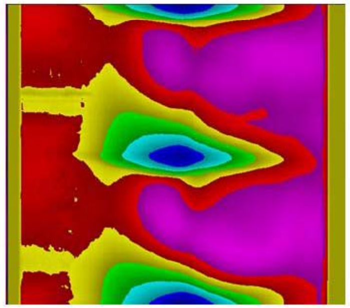

Model Validation

Plug # 3

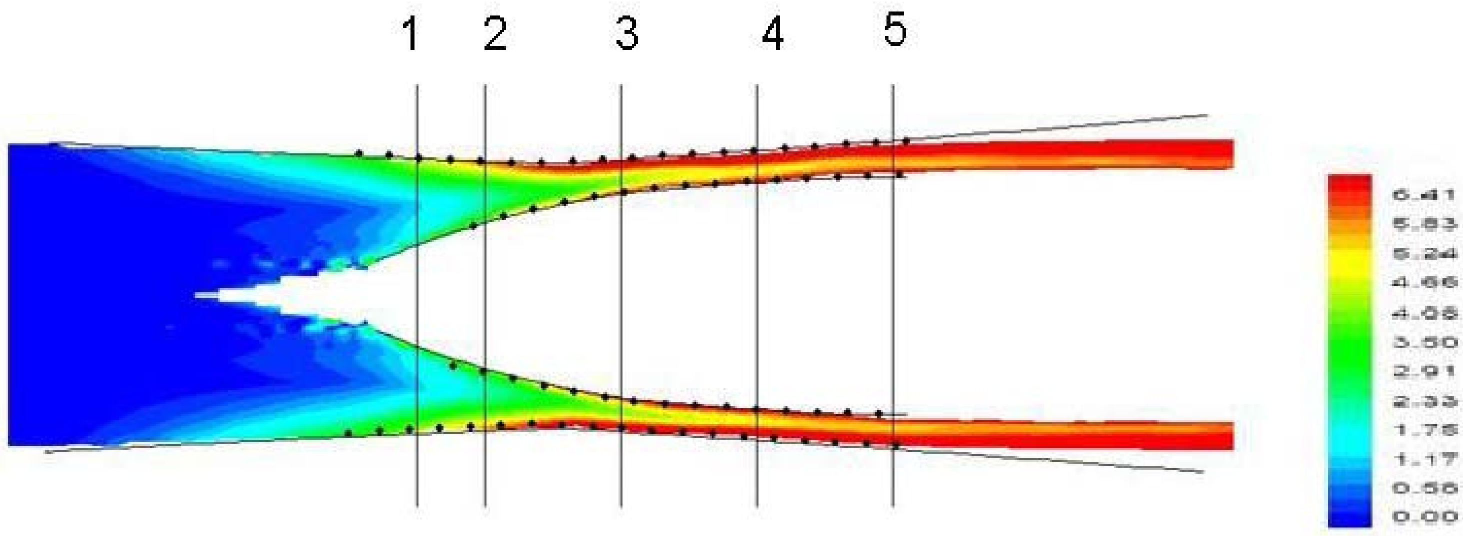

Model Validation

Plug # 3

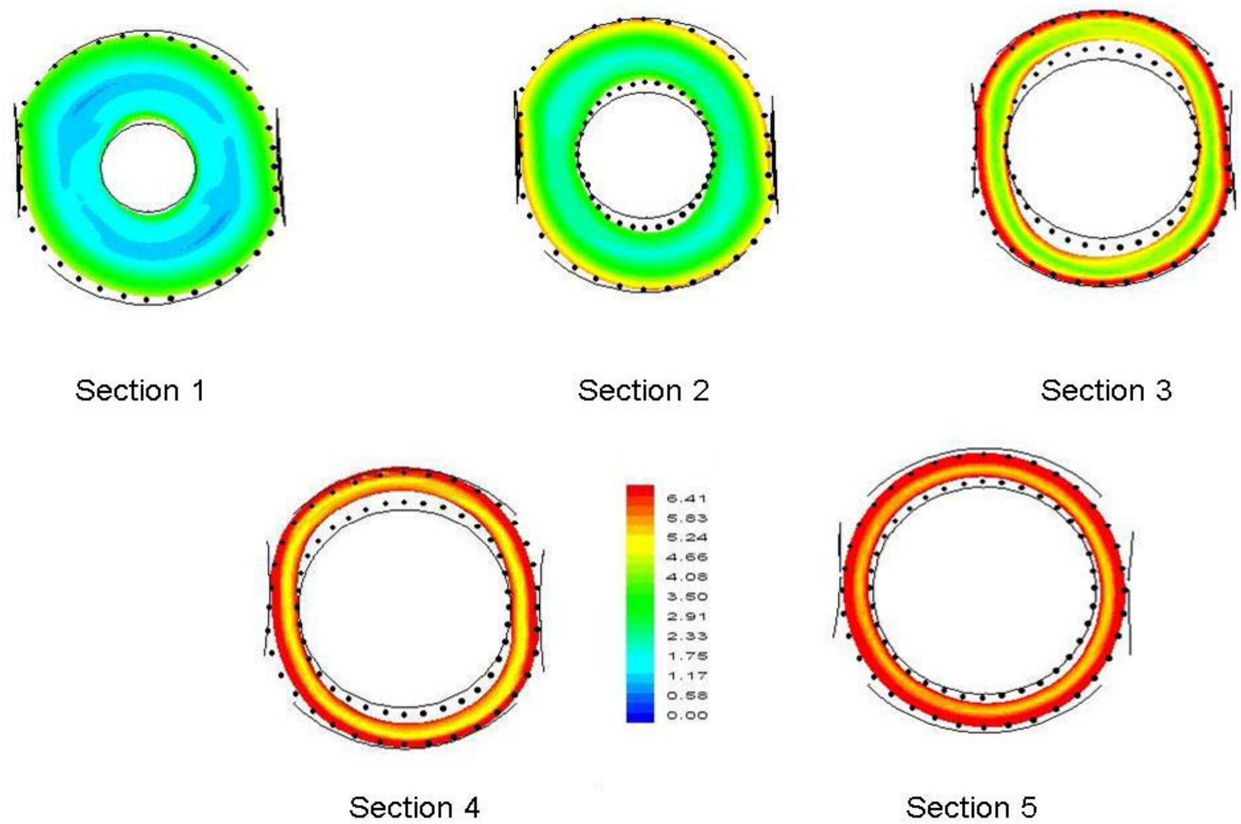

Model Validation

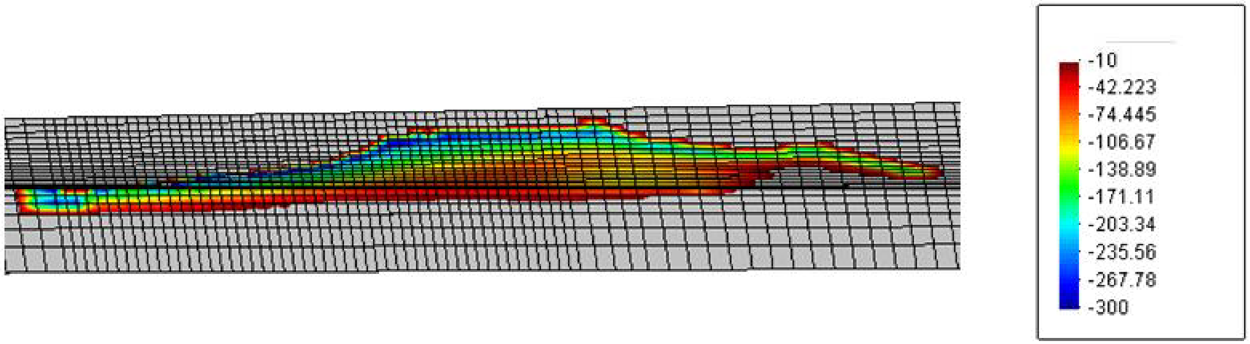

Contact Pressure [Mpa]